Published in final edited form as:

J Immunol. 2016 August 15; 197(4): 1035–1043. doi:10.4049/jimmunol.1500654.

ERAAP shapes the peptidome associated with classical and non-classical MHC class I molecules[1]

Niranjana A. Nagarajan[*,2,††], **Danielle A. de Verteuil**[†], **Dev Sriranganadane**[†], **Wafaa Yahyaoui**[†], **Pierre Thibault**[†], **Claude Perreault**[†], and **Nilabh Shastri**[*,2]

[*]Division of Immunology and Pathogenesis, Department of Molecular and Cell Biology, University of California, Berkeley, CA 94720, USA

[†]Institute for Research in Immunology and Cancer, Université de Montréal, Montreal, QC, Canada H3C 3J7

Abstract

The peptide repertoire presented by classical as well as non-classical MHC I molecules is altered in the absence of the ER aminopeptidase associated with antigen processing (ERAAP). To characterize the extent of these changes, peptides from cells lacking ERAAP were eluted from the cell surface and analyzed by high-throughput mass spectrometry. We found that the majority of peptides found in WT cells were retained in the absence of ERAAP. In contrast, a subset of "ERAAP-edited" peptides was lost in WT cells, and ERAAP-deficient cells presented an unique "unedited" repertoire. A substantial fraction of MHC-associated peptides from ERAAP-deficient cells contained N-terminal extensions and had a different molecular composition than those from WT cells. We found that the number and immunogenicity of peptides associated with non-classical MHC I was increased in the absence of ERAAP. Conversely, only peptides presented by classical MHC I were immunogenic in ERAAP-sufficient cells. Finally, MHC I peptides were also derived from different intracellular sources in ERAAP-deficient cells.

Keywords

Antigen Processing; MHC class I; autoimmunity

[1]This work was supported by grant # 701564 from the Canadian Cancer Society Research Institute (to C.P. and P.T.) and by grants from the NIH to N.S. N.A.N. was supported in part by the Irvington Institute Fellowship program of the Cancer Research Institute. D.de V. was supported by a doctoral research award from the Fonds de Recherche Québec Santé. C.P. and P.T. hold Canada Research Chairs in Immunobiology, and Proteomics and Bioanalytical Spectrometry, respectively.

[2]Address correspondence to Nilabh Shastri, Phone: +1-510-643-9197, Fax: +1-510-643-9230, nshastri@berkeley.edu, Or Niranjana Nagarajan: niranjana.nagarajan@icloud.com.

[††]Present address : Adheren Inc. 5858 Horton Street, Suite 255, Emeryville, CA 94608

Author Contributions

N.A.N, D. de V, P.T., C.P. and N.S. designed the study, N.A.N, D.de.V, D.S. and W.Y. carried out the experiments and analyzed the data, N.A.N and N.S. wrote the manuscript with inputs from all the other authors.

The authors declare that they have no competing financial interests.

Introduction

MHC class I molecules present peptides to CD8 T cells, for recognition by their T cell receptors (1–3). CD8 T cells are tolerant to the "self" peptide-MHC I (pMHC I)[3] complexes present at steady state on the cell surface, and are activated when infected or transformed cells present either foreign or "altered-self" peptides. An essential part of immune surveillance is the recognition and elimination of infected or transformed cells by cytotoxic CD8 T cells. However, inappropriate recognition of pMHC I complexes and consequent activation of CD8 T cells can result in autoimmune disease.

The generation and loading of peptides onto MHC class I are tightly regulated, to prevent unintended activation of CD8 T cells (1–3). The failure of this regulation, and impairment of components of the antigen processing pathway, can lead to the presentation of novel immunogenic peptide-MHC I complexes and possible autoimmunity (4). The ER aminopeptidase associated with antigen processing (ERAAP,(5)) edits the N-termini of peptides presented by MHC I molecules after transport into the ER by the transporter associated with antigen processing (TAP(2)). Polymorphic variants of human ERAAP have been associated with a variety of autoimmune diseases (6–11), suggesting that ERAAP strongly influences the peptides presented by MHC I molecules. Indeed, changes in the pMHC I repertoire associated with ERAP1 polymorphisms have been found (12).

The association of ERAAP with many different autoimmune diseases suggests that there may be differences in metabolic and cellular pathways in ERAAP-deficient cells that could predispose the host to autoimmunity. Additionally, using a mouse model for ERAAP deficiency (13), we have found that the loss of ERAAP results in significant alterations in the peptides presented by both classical, or MHC class Ia (MHC Ia) and non-classical, or MHC class Ib (MHC Ib) molecules, resulting in robust CD8 T cell responses (14, 15). We therefore decided to analyze the MHC I-associated peptide repertoire in the absence of ERAAP using high throughput peptidomics (16, 17), to determine both the molecular changes in peptide presentation and the systemic cellular changes that might occur as a result of ERAAP deficiency.

In this study, we present a global analysis of the peptides presented by MHC class I molecules on the cell surface when ERAAP is absent. We found that ERAAP-deficient cells presented a larger number of peptides bound to non-polymorphic MHC Ib molecules, and that both MHC Ia and MHC Ib molecules on these cells presented longer peptides. A substantial number of peptides were unaffected by the absence of ERAAP while another set of peptides was not detected in ERAAP-deficient cells, suggesting that ERAAP is essential for generating a distinct subset of peptides. Interestingly, a set of new unedited peptides was present on ERAAP-deficient cells but was not detected in wild-type cells. Additionally, a large fraction of the unedited peptides were Qa-1^b -associated and the CD8+ T cell response of WT mice to ERAAP-deficient cells was largely Qa-1^b restricted.

[3]Abbreviations used in this paper: pMHC I (peptide MHC class I), BMDC (bone marrow derived dendritic cells), ERAAP (ER aminopeptidase associated with antigen processing), MS (mass spectrometry), GO (gene ontology), SP-PIR (Swiss-Prot-Protein Information Resource)

This large dataset also allowed us to identify the general characteristics and sources of ERAAP-dependent MHC I associated peptides (18, 19). We found that peptides presented on ERAAP-deficient cells were derived from a different constellation of proteins compared to WT cells. A peptide from the *Fbxl19* gene was presented specifically by ERAAP-deficient cells, and elicited a CTL response in WT mice. Because GWAS studies of psoriasis patients have linked both the *Fbxl19* and *ERAP1* genes to the disease (6, 7), the discovery of an immunogenic *Fbx19*-derived peptides on ERAAP-deficient suggests a potential mechanism driving pathogenesis of psoriasis.

Materials and Methods

Mice

ERAAP$^{-/-}$ mice (B6.129.*Arts1*^{tm1Ucb}) have been previously described. ERAAP$^{-/-}$K^{b}D$^{b-/-}$, ERAAP$^{-/-}$TAP$^{-/-}$, ERAAP$^{-/-}\beta_2$m$^{-/-}$ and ERAAP$^{-/-}$ Qa-1$^{b\ -/-}$ mice were generated in our facility by crossing the respective knockout mice with ERAAP$^{-/-}$ mice. WT C57Bl/6J, and β_2m$^{-/-}$ mice were either purchased from the Jackson Laboratory (Bar Harbor, ME) or bred in our facility. Qa-1$^{b\ -/-}$ mice were generated in the laboratory of Dr. Harvey Cantor (Harvard University) and were the kind gift of Dr. Edgar Engleman (Stanford University). Mice were housed and all procedures carried out with the approval of, and in accordance with, the institutional animal care guidelines of the University of California Berkeley and the University of Montreal.

MHC I-peptide extraction and MS analyses

MHC I-peptides were isolated from BMDCs as described previously using mild acid elution (Fortier *et al*, 2008). Two biological replicates (500 × 10^6 BMDCs per replicate) were prepared. MHC I-peptides obtained after acid elution were separated using an off-line 1100 series binary LC system (Agilent Technologies) to remove contaminating species. Peptides were loaded on a homemade strong cation exchange (SCX) column (0.3 mm internal diameter × 50 mm length) packed with SCX bulk material (Polysulfoethyl ATM, PolyLC). Peptides were fractionated with a gradient of 0–25% B after 25 min, 25–60% B after 35 min (solvent A: 5 mM ammonium formate, 15% acetonitrile, pH 3.0; solvent B: 2 M ammonium formate, 15% acetonitrile, pH 3.0). MHC I-peptides were collected in five consecutive fractions and brought to dryness using a speedvac. Peptide fractions were resuspended in 2% aqueous acetonitrile (0.2% formic acid) and analyzed by nanoLC–MS/MS on a LTQ-Orbitrap Velos mass spectrometer (Thermo Fisher Scientific). Full mass spectra were acquired with the Orbitrap analyzer operated at a resolving power of 60 000 (at m/z 400) and collision-activated dissociation tandem mass spectra were acquired in data-dependent mode with the quadrupole linear ion trap analyzer. Mass calibration used an internal lock mass (protonated (Si(CH$_3$)$_2$O))6; m/z 445.120025) and typically provided mass accuracy within 5 p.p.m. for all nanoLC–MS/MS experiments.

MS/MS sequencing, hierarchical clustering and identification of MHC I peptide-source proteins

Peptidomic data were analyzed using Xcalibur software and peak lists were generated using Mascot distiller (version 2.1.1, http://www.matrixscience.com). Database searches were

performed against the International Protein Index mouse database (version 3.23 containing 51,536 sequences and 24,497,860 residues) using Mascot (version 2.2, http://www.matrixscience.com) with a mass precursor tolerance of 15 ppm and a fragment tolerance of ±0.5 Da. Searches were performed without enzyme specificity with variable modifications for oxidation (Met) and deamidation (Asn, Gln). Label-free quantitative proteomics was used to compare peptide abundance across sample sets as described previously (de Verteuil *et al*, 2010). Briefly, peptide maps were aligned and clustered together to profile the abundance of Mascot identified peptides using hierarchical clustering with criteria based on *m*/*z* and time tolerance (±0.02 *m*/*z* and ±1 min). This resulted in a list of non-redundant peptide clusters for both replicates of all samples. The list of all peptides and their source proteins is available from the Immune Epitope Data Base under the accession number 1000706 (http://www.iedb.org/SubID/1000706)

MHC I-specific peptides were determined by comparing peptides from WT and ERAAP-KO eluates to the β_2m-KO negative control. In order to keep as much as possible of the MHC I-peptides (avoid false negatives), a cutoff of 2-fold was used when comparing the intensity of peptides that were detected in both β2m replicates to the intensity detected in WT or in ERAAP-KO (Fortier *et al*, 2008), with a permissive p-value of less than 0.1 since only two replicates were included in the analyses. Peptides that were detected only in one or none of the β_2m replicates were also considered as MHC I-associated peptides. In order to identify peptides specific to WT, specific to ERAAP-KO or common to both conditions, we only selected those with at least 5-fold change in abundance. Peptides that were below threshold were given an intensity value of 8,000. WT-specific peptides were identified as those detected in both WT replicates and in either one or two replicates of ERAAP-KO (with a WT / ERAAP-KO fold change > 5, and $p < 0.1$), or not detected in either ERAAP-KO replicates. The same treatment was used to determine ERAAP-KO-specific peptides. Common peptides were those detected in both WT and both ERAAP-KO replicates, with a calculated fold-change intensity lower than 5 ($p > 0.1$).

Finally, Qa1-associated peptides were identified as those detected in both ERAAP-KO replicates and in either one or two replicates of Qa-1^b -ERAAP-dKO (with an ERAAP-KO / Qa-1-ERAAP-dKO fold change intensity > 5, and $p < 0.1$), or not detected in either Qa-1-ERAAP-dKO replicates.

Antibodies and peptides

Antibodies for flow cytometry were obtained from BD Biosciences (CD8α, CD4, B220, TCRβ, CD44, NK1.1, Qa-1^b, CD11c, H2-K^b, H2-D^b, I-A^b and IFNγ) and BioLegend (CD62L). All peptides were synthesized by Dr. David King (UC Berkeley).

Analysis of peptide-MHC binding and motifs

Peptide binding affinity for H2-K^b and H2-D^b were determined using the NetMHC algorithm (20). Peptides between 8 and 14 residues in length were analyzed, and those with a predicted IC50 of 500nM or less were classified as good binders. Peptides 9 residues and longer were analyzed using the Rankpep algorithm (21, 22) to determine Qa-2^a binding

peptides. All peptides with a core region that had positive score were assigned as Qa-2^a - associated. Peptides with C-terminal extensions of the core region were excluded.

CTL and T cell activation assays

WT anti-ERAAP-KO CD8 T cells lines were generated by immunizing C57Bl/6J mice once with 2X10^7 ERAAP$^{-/-}$ spleen cells intraperitoneally. ERAAP-KO anti-WT CD8 T cell lines were generated by immunizing ERAAP-KO mice once with 2X10^7 C57BL/6J spleen cells intraperitoneally. Spleens were harvested from immunized mice ten days after immunization. 5X10^6 responder spleen cells were restimulated *in vitro* with an equal number of irradiated stimulator spleen cells, which were the same genotype as used to immunize, with 20 U/ml of recombinant human IL-2 (National Cancer Institute) per well in 24-well plates. T cells were used for IFNγ assays six days after restimulation. To measure intracellular IFNγ, CD8 T cell lines were harvested and stimulated for 5h with CD4-and CD8-depleted LPS-blasted spleen APCs of the indicated genotypes. Golgi-Plug (BD Biosciences) was added for the latter four hours of the incubation period. Cells were then stained first with surface markers, or with tetramers followed by other surface markers, fixed, permeabilized, and stained for intracellular IFNγ. For *ex vivo* analysis of IFNγ production, spleen cells were harvested from immunized mice and plated in 96-well plates with 1 μM of the indicated peptides for 5h in the presence of Golgi-Plug. The cells were then stained as described.

Analysis of GO terms and protein function keywords

The gene symbols for the source genes for WT-, ERAAP-KO-specific, or common peptides were annotated and analyzed using DAVID (http://david.abcc.ncifcrf.gov/; (23)). The background for each set was set as the group of gene symbols in the mouse genomic informatics (MGI) database. Only the group of gene symbols with corresponding annotations in DAVID were analyzed. The EASE threshold was set as 0.01, and gene ontology terms describing cellular components (GO-CC) and protein function keywords (SP-PIR) preferentially enriched for each group were determined. Terms or keywords with a false discovery rate of >5% were excluded. GO terms and keywords which were associated uniquely with ERAAP-KO peptides, and not with WT or common peptides were determined.

Results

Global changes in MHC I associated peptides in ERAAP-deficient cells

Our earlier work has shown that unedited peptides are presented by the MHC Ia molecules H2-K^b and H2-D^b in the absence of ERAAP (24). However, that analysis of immunoprecipitated MHC I molecules from lysed cells could not distinguish between cell surface pMHC I and intracellular intermediates. Furthermore, the absence of ERAAP results in conformational changes in both MHC Ia- and MHC Ib-associated peptides (14, 15), which may not be recognized by conventional antibodies raised against WT MHC class I molecules. To circumvent these concerns, we used mild acid treatment to potentially elute all peptides from the surface of WT (16), ERAAP-deficient (ERAAP-KO), and Qa-1^b - and ERAAP-double deficient (Qa-1-ERAAP-DKO) bone marrow-derived dendritic cells

(BMDCs). Peptides were separated by liquid chromatography and sequenced by tandem mass spectrometry, as previously described (Table I, http://www.iedb.org/SubID/1000706) , (16, 18). Peptides eluted from the surface of β2-microglobulin-deficient (β_2m-KO) BMDCs were used to exclude MHC I-independent, non-specific peptides.

We defined peptides as specific to WT or ERAAP-deficient cells if they were unique (Fig. 1A) to either condition, or overexpressed (> 5 fold, $p < 0.1$, Fig. 1B) in one sample versus another. Common peptides were defined as those found in both WT and ERAAP-deficient cells with a less than 5-fold difference in intensity between WT and ERAAP-deficient cells (Fig. 1B). We identified 2367 peptides common to both WT and ERAAP-deficient cells (common peptides), 440 specific to WT cells (WT-specific peptides; 269 unique (Fig. 1A) plus 171 overexpressed (Fig. 1B)) and 389 specific to ERAAP-deficient cells (ERAAP-KO-specific peptides; 184 unique (Fig. 1A) plus 205 overexpressed (Fig. 1B); Table I, complete lists of peptides are at http://www.iedb.org/SubID/1000706).

Algorithms for identifying Qa-1^b associated peptides are not available, and the peptide-binding motif is poorly defined. We therefore used a subtractive strategy to determine the sequences of Qa-1^b -associated peptides from ERAAP-deficient cells. We compared the peptides isolated from Qa-1^b and ERAAP-double deficient BMDCs, and compared the results to those from BMDCs deficient only in ERAAP. As described earlier, peptides that were detected in ERAAP-deficient cells but not in Qa-1^b and ERAAP-double deficient cells, or that were detected at intensities five-fold, or higher, in ERAAP-deficient cells ($p < 0.1$), were designated as ERAAP-KO-specific Qa-1^b -associated peptides (Fig. 2, http://www.iedb.org/SubID/1000706). We found 232 Qa1-associated peptides (133 unique and 99 overexpressed, Fig. 2A). 73 of these peptides were detected in both replicates as associated with ERAAP-KO but only in single replicates as associated with WT. We could therefore assign them as unambiguously present only in ERAAP-KO, and excluded these peptides from our further analyses. Similarly, we identified WT-specific Qa-1^b -associated peptides as those found only in, or overexpressed by, WT cells, when compared to both ERAAP-KO and Qa-1-ERAAP-DKO cells. Common Qa-1^b -associated peptides were those found in, or overexpressed by, both WT and ERAAP-deficient cells, when compared to Qa-1^b -ERAAP-double deficient cells. We found 86 Qa-1^b -associated peptides common to both WT and ERAAP-KO cells, 6 specific to WT cells, and 67 peptides specific to ERAAP-KO cells (http://www.iedb.org/SubID/1000706).

Longer peptides are presented on the cell surface in the absence of ERAAP

We analyzed the distribution of the lengths of ERAAP-KO- and WT-specific and common peptides, and found that peptides eluted from ERAAP-deficient cells were longer than those specific to WT cells, or common to both ($p=0.0122$, one way ANOVA) (Fig. 1C). Since our analysis is specific to cell surface pMHC I complexes, and not to potential intracellular intermediates, we conclude that MHC I molecules present longer peptides on the cell surface in ERAAP-deficient cells.

We then analyzed specifically whether MHC class Ia- or MHC class Ib-associated peptides were longer in ERAAP-deficient cells. Non- Qa-1^b -associated peptides were analyzed using the NetMHC algorithm (20), to predict their binding affinity to H2-K^b and H2-D^b, the MHC

Ia molecules expressed by the H-2^b haplotype. NetMHC classifies peptides as strong MHC binders when their predicted IC_{50} is less than 50nM, whereas weak binders correspond to those with IC_{50} less than 500nM. We therefore used an IC50 of 500nM as the cutoff, to classify peptides as H-2K^b or H-2D^b binders (http://www.iedb.org/SubID/1000706). In this subset of peptides identified as good MHC binders, we found that the majority of WT-specific and common peptides were of the canonical length—8 residues for H2-K^b binders and 9 residues for H2-D^b binders (Fig. 1D–E). Strikingly, we found that a lesser proportion of the ERAAP-KO-specific good MHC binders were of the canonical length (Fig. 1D–E). Indeed, the majority of the ERAAP-KO specific good MHC binders were longer than 8 (for H2-K^b, Fig. 1D) or 9 (for H2-D^b, Fig. 1E) amino acid residues. These results show that ERAAP-deficient cells present longer peptides overall, and that these longer peptides were predicted to bind to MHC I with an affinity of less than 500nM.

To identify peptides associated with Qa-2^a, a non-classical MHC I molecule, we analyzed all peptides 9 residues in length or longer by the Rankpep algorithm (21, 22) (Fig. 1F, http://www.iedb.org/SubID/1000706, Fig. S2). Rankpep defines a core region for Qa-2^a binding, and includes longer peptides that have either N- or C-terminal extensions to this core region. We excluded peptides with C-terminal extensions, since Qa-2^a, like conventional MHC I molecules, is known to require a hydrophobic residue at the C-terminus (25–27). Moreover, C-terminal extensions have been found to be deleterious for MHC I binding (28). We identified 169 Qa-2^a -associated peptides common to both ERAAP-KO and WT cells, 29 specific to WT and 24 specific to ERAAP-KO (Table I, http://www.iedb.org/SubID/1000706). Weblogo analysis of the amino acid composition of these predicted Qa-2-associated peptides confirmed the presence of the characteristic histidine at position 7 of the peptide (Fig. S2). No clear motif emerged from an analysis of the N-termini of these peptides (Fig. S2). Strikingly, when we analyzed the lengths of these predicted Qa-2^a associated peptides, we found that ERAAP-KO-specific peptides were longer (Fig 1F). These results suggest that the generation of the peptide repertoire presented by Qa-2^a is also strongly influenced by ERAAP.

Qualitative and quantitative changes in Qa-1^b -associated peptides in ERAAP- deficient cells

Relatively little is known about the peptide-binding preferences of the MHC class Ib molecule Qa-1^b. There have been very few Qa-1^b -binding peptides definitively identified to serve as T cell ligands (29–33), and the numbers of endogenous peptide sequences are insufficient to derive general rules for the peptide-binding preferences of Qa-1^b. When comparing peptides isolated from WT and ERAAP-deficient cells to those isolated from Qa-1^b and ERAAP double-deficient cells, our subtractive strategy identified numerous endogenous peptides associated with Qa-1^b (Fig. 2A-B, http://www.iedb.org/SubID/1000706).

86 peptides were found to be Qa-1^b -associated (i.e., absent in Qa-1-ERAAP-DKO cells) and common to Qa-1^b + WT and ERAAP-deficient cells. The current analysis cannot unambiguously assign WT-specific Qa-1^b peptides, since Qa-1-KO ERAAP WT cells were not tested. However, 67 Qa-1^b -associated peptides were identified from ERAAP-deficient

cells, while only 6 Qa-1^b -associated peptides were found in WT cells, and not ERAAP-deficient (Table I, Fig. 2A-B, http://www.iedb.org/SubID/1000706), suggesting that more peptides are presented by Qa-1^b in the absence of ERAAP. Notably, we did identify the Qdm peptide (30), derived from the leader sequence of H2-D^b, in WT cells, and to a lower extent in ERAAP-deficient cells in agreement with an earlier study (34). However, this peptide did not meet our filtering criteria for inclusion in our main analysis, since it was not found at amounts more than five-fold higher in WT compared to ERAAP-KO (http://www.iedb.org/SubID/1000706).

We identified Qa-1^b -associated peptides ranging from 6-24 residues in length (Table I, http://www.iedb.org/SubID/1000706). Since there were only six WT-specific Qa-1^b -associated peptides, three of which were 8 residues long and three that were 9 residues long, they were analyzed together with the common peptides, called combined common and WT peptides (Fig. 2C). Focusing on peptides between 6 and 15 residues in length, we found that the majority of Qa-1^b -associated peptides common to WT and ERAAP-deficient cells were nine residues long, in agreement with the canonical length of most MHC-associated peptides. However, consistent with MHC Ia- and Qa-2^a -associated peptides (Fig. 1C–F), Qa-1^b -associated peptides on the surface of ERAAP-deficient cells were also longer, with the majority of these peptides being ten residues long (Fig. 2C).

We then analyzed the amino acid composition of the Qa-1^b -associated peptides using weblogos (Fig. 2D). The results are presented as frequency plots, where the size of the single letter amino acid symbol is in proportion to the frequency of its occurrence at that position. To determine a peptide binding motif, we analyzed the complete sequences of all the nine-residue long peptides from the combined WT and common peptide set, as these are the endogenous peptides of the canonical length found at steady-state (Fig. 2D, upper left panel). These peptides showed a strong preference for a hydrophobic residue (leucine, isoleucine or valine) at the C-terminus (P9) and a similar preference for a hydrophobic aliphatic residue (leucine, valine or alanine) at P3 from the N-terminus, and either asparagine or arginine at P5. In contrast to prior analyses of substituted Qdm peptides (35), we found no preference for a methionine at P2, suggesting that this position may not be an anchor position.

Remarkably, none of these preferences were retained in Qa-1^b -associated peptides from ERAAP-deficient cells, or from common peptides 10 residues long (Fig 2D, upper right and lower panels). Likewise, no strong amino acid preferences were evident at the C-termini of 10-residue long common peptides, or in the ERAAP-KO-specific peptides, although the common 10-residue long peptides and ERAAP-KO-specific 9-mers retained a preference for a hydrophobic aliphatic residue at P3. Ten-residue long ERAAP-KO-specific peptides showed a preference for either leucine or valine at P4, in common with 10-residue long common peptides, which showed a preference for leucine at P4.

These findings suggest that Qa-1^b has a permissive peptide-binding motif, with a preference for hydrophobic amino acids at P3 and the C-terminus, and for canonical nine-residue long peptides. Nevertheless, peptides longer than the canonical nine residues, and peptides specific to ERAAP-KO cells are presented despite not conforming to this motif.

ERAAP edits a subset of peptides, generating a unique N-terminus

We have previously established that the aminopeptidase ERAAP plays a crucial role in trimming the N-termini of peptides that are eventually presented by MHC I (5). We wanted to determine whether the absence of ERAAP resulted in a global change in the nature of the N-termini of MHC I-associated peptides. We therefore analyzed the amino acid composition of the N- and C-termini of the isolated peptides, using weblogos (36) (Figs. 3 and S1). All the peptides were aligned at their C-termini, and their sequences analyzed from the C-terminus to the -5 position (Fig S1). The analysis clearly showed that all the peptides (WT- and ERAAP-KO-specific, and common peptides) had the canonical hydrophobic C-termini (Fig. S1).

We then aligned all the peptides at their N-termini, and analyzed the composition of the first six amino acids (Fig. 3A). Intriguingly, we found that ERAAP-KO-specific peptides and the common peptides appeared to have a similar distribution of amino acids at their N-termini (Fig. 3A, center and lower panels). Strikingly, WT-specific peptides had a different amino acid composition from either common or ERAAP-KO-specific peptides (Fig. 3A, upper panel). WT peptides appeared to have a preference for hydrophobic residues at five of the six N-terminal positions we analyzed. This distinctive preference for hydrophobic residues in the N-terminal profile is absent in common peptides and in those from ERAAP-deficient cells.

This is especially evident at the N-terminal residue, which would be generated by ERAAP cleavage (Fig. 3B, C). The relative frequencies of each amino acid at the N-terminus were determined by subtracting the frequency of occurrence in common peptides from WT- or ERAAP-KO-specific peptides (Fig. 3B). WT-specific peptides have Ile, Leu or Val more frequently at this position, while ERAAP-KO peptides have Ala and Ser. Conversely, WT peptides have Ser and Ala much less frequently than common peptides (Fig. 3B). To visualize this trend more clearly, the relative frequencies of N-terminal amino acids in common and ERAAP-KO-specific peptides were determined relative to WT-specific peptides (Fig. 3C). The pattern of usage of individual amino acids by ERAAP-KO-specific and common peptides relative to WT is highly similar, with less frequent occurrences of hydrophobic residues Ile, Leu and Val, and more frequent occurrence of Ala and Ser.

The strong similarity in amino acid preferences between the N-termini of the common and ERAAP-KO-specific peptides suggests that these peptides were generated in a manner that did not require ERAAP. We conclude that these peptides represent the repertoire of peptides unedited by ERAAP.

Differential immunogenicity of pMHC Ia versus pMHC Ib complexes due to ERAAP activity

Given the striking changes in both MHC Ia- and MHC Ib-associated peptides in the absence of ERAAP, we wanted to test the relative immunogenicity of pMHC Ia versus pMHC Ib expressed by WT and ERAAP-KO cells. ERAAP-deficient mice were immunized with spleen cells from WT mice, and responding ERAAP-KO anti-WT T cells expanded by restimulation *in vitro* with irradiated WT splenic APCs (Fig. 4A). IFNγ production by these CD8 T cell lines was measured in response to self (ERAAP-KO), WT, MHC Ia-deficient

(H2-K^b-H2-D^b-DKO), Qa-1^b -deficient APCs (Qa-1-KO), and APCs lacking peptide transport into the ER (TAP-KO). Conversely, WT mice were immunized with ERAAP-deficient cells, and responding WT-anti-ERAAP-KO CD8 T cells were tested for their responses to self (WT) APCs, and ERAAP-deficient, ERAAP and MHC Ia-, Qa-1^b - and TAP-deficient cells (Fig. 4B).

As previously reported (14, 15), we found that WT anti-ERAAP-KO CD8 T cells recognized both MHC Ia-sufficient and MHC Ia-deficient ERAAP-deficient APCs (Fig. 4B). WT anti-ERAAP-KO CD8 T cells required conventional peptide transport because they did not respond to TAP-deficient ERAAP-deficient APCs. WT anti-ERAAP-KO T cells also showed reduced responses to Qa-1^b -deficient ERAAP-deficient APCs, suggesting that a large proportion of WT CD8 T cells respond to immunogenic peptide- Qa-1^b (p- Qa-1^b) complexes (Fig. 4A). In contrast, we found that CD8 T cells in ERAAP-deficient mice mounted a vigorous response against WT APCs (Fig. 4B), but did not respond to MHC Ia-deficient and TAP-deficient APCs, indicating that they did not recognize peptides presented by MHC Ib molecules on WT cells as foreign. The response of ERAAP-KO-anti-WT CTLs to Qa-1^b -deficient APCs was also unimpaired (Fig. 4B), suggesting that WT APCs did not present immunogenic peptide- Qa-1^b complexes to ERAAP-deficient CD8 T cells.

These results show that despite clear global changes in the pMHC Ib and pMHC Ia complexes presented by ERAAP-deficient cells, the relative immunogenicity of these changes is distinct: WT mice respond to immunogenic pMHC Ia and pMHC Ib complexes on ERAAP-deficient cells, but ERAAP- deficient mice respond exclusively to immunogenic pMHC Ia complexes.

MHC I peptides arise from different protein sources in ERAAP-deficient cells

We have previously shown that the pMHC I repertoire on the cell surface is a direct representation of the transcriptional and physiological state of the cell (18, 19). The sources of cell surface pMHC I change with the cellular state— for example, transformed cells present peptides encoded by genes characteristic of neoplastic transformation (16), while cells treated with rapamycin present peptides encoded by genes involved in mTOR signaling (19). Furthermore, a substantial proportion of MHC I-peptides are cell type-specific (18). To test whether the absence of ERAAP led to the processing and presentation of peptides encoded by unique subsets of genes we analyzed the source genes of MHC I-associated peptides from WT or ERAAP-deficient cells.

We used the DAVID database (Database for Annotation Visualization and Discovery, (23)) to analyze lists of gene symbols for source genes for MHC I-associated peptides specific to WT or ERAAP-deficient cells, or common to both. We used a highly restrictive EASE threshold of 0.01 to filter our results, and only counted results that had a false discovery rate of less than 5%. We focused our analysis on two areas: gene ontology (GO) terms that described cellular components, and protein function (SP-PIR) keywords.

We looked for the GO terms and keywords that were preferentially enriched in source genes for common, WT-specific and ERAAP-KO-specific peptides compared to the background set of all the genes in the Mouse Genome Informatics (MGI) database. The complete lists of

GO terms and keywords we found preferentially enriched in the three sets are listed in Table s2. Some GO terms and keywords appear to be generally characteristic of pMHC I presented on the surface of BMDCs—for example, 44-51% peptides in all three sets derived from phosphoproteins (Table S1). Since phosphorylation is often a prerequisite for ubiquitylation and targeting for degradation (37), this enrichment could reflect the nature of MHC I-associated peptides in general. We then filtered the list of GO terms and keywords uniquely associated with either the WT or ERAAP-KO set against the GO terms and functional keywords associated with common peptides, to generate a list of GO terms and keywords specifically associated with peptides derived from ERAAP-deficient cells (Table II).

The analysis of GO terms showed that a fraction of MHC I peptides from ERAAP-deficient cells were preferentially derived from proteins from the Golgi (Table II). These observations are consistent with the idea that MHC I peptides can be processed in other compartments when ER processing is compromised (38). The pool of optimally trimmed MHC I peptides is reduced in ERAAP-deficient cells, as we, and others, have shown. As a consequence, pMHC I complexes that exit the ER in ERAAP-deficient cells are less stable, and might be more susceptible to exchange with peptides of higher affinity, generated in post-ER cell compartments.

Analyzing the protein function keywords associated with ERAAP-KO-specific peptides showed that the keywords “wd repeat”, “methylation” and “leucine-rich repeat (LRR)” were specifically enriched (Table II). Of these keywords, only leucine-rich-repeat was entirely unique to ERAAP-KO-specific peptides, since the other keywords were found in the other lists, albeit without reaching statistical significance (Table S1). We noticed that one of the peptides presented specifically in ERAAP-deficient cells was derived from the LRR-containing protein Fbxl19 (Table S1). Strikingly, the human *FBXL19* gene has been associated with psoriasis in genome-wide association studies, which have also linked ERAP1, the human homolog of ERAAP, to psoriasis (6, 7).

To determine whether the preferential enrichment of the Fbxl19-derived DPSVHLLTA (DA9) peptide in our analyses was actually immunogenic, WT B6 mice were immunized with ERAAP-KO spleen cells and immune responses measured by intracellular IFNγ production in response to synthetic peptides directly *ex vivo* (Fig. 5). Remarkably, B6 anti-ERAAP-KO (BEko) immunized mice mounted robust responses to the DA9 peptide *ex vivo*. CD8 T cells from immunized, but not naïve mice, downregulated L-selectin (CD62L), a marker of activation, and produced IFNγ when restimulated *ex vivo* with the DA9 peptide (Fig 5A,B). As a positive control, we detected responses in the same mice against the FL9 peptide derived from the Fam49b protein, as shown previously (15). Naïve mice, or immunized mice restimulated without peptide did not produce IFN7gamma; (Fig. 5). Thus, among the many different peptides presented by ERAAP-KO cells, the DA9 peptide appears to induce an immunodominant T cell response. These results demonstrate a clear molecular link between presentation of an Fbxl19-derived peptide and the absence of ERAAP function in autoimmune disease

Discussion

We used a combination of high-throughput mass spectrometry and bioinformatics to analyze the changes in the pMHC I repertoire that occur when N-terminal peptide trimming by ERAAP is lost. The differences between the WT and ERAAP-deficient pMHC I repertoire are extensive and diverse, and encompass both the highly polymorphic MHC Ia molecules and the non-polymorphic MHC Ib molecules. The flexibility of our method, which isolates all cell surface MHC I-associated peptides regardless of whether they can be recovered by immunoprecipitation, allowed us to analyze common peptides found in both WT and ERAAP-deficient cells and those found specifically in WT or ERAAP-deficient cells. It is clear that MHC Ia- and MHC Ib-associated peptides specific to ERAAP-deficient cells are longer, compared to either the common or WT-specific peptides. This analysis provides insights into the role of N-terminal trimming in shaping the peptide repertoire presented by both MHC Ia and MHC Ib molecules.

ERAAP-KO-specific peptides have the canonical hydrophobic C-termini, yet are not simply N-terminally extended precursors of WT-specific peptides. Instead, ERAAP-KO-specific peptides showed a N-terminal pattern of amino acid usage strikingly similar to that of peptides common to both strains. The N-termini of WT-specific peptides, however, showed a clearly distinct pattern of amino acids, with a preference for hydrophobic amino acids at five out of six positions. This observation is especially striking at P1, the first residue of the peptide, and the one generated as a direct result of ERAAP cleavage. These results suggest that ERAAP generates a specific subset of peptides with a preference for certain N-terminal residues, consistent with the work of Schatz et al, in which it was shown that peptides with serine at the N-terminus are much less susceptible to endoplasmic aminopeptidase cleavage (39). When ERAAP is absent, this subset is no longer edited and is lost. The bulk of MHC I associated peptides thus have the ERAAP “unedited” N-termini similar to those observed in the common set of peptides. These observations suggest that ERAAP plays a role in processing a subset of, but not all, peptides for presented by MHC I.

Our analyses provided several interesting insights into the global MHC Ib-associated peptide repertoire. We found that similar to the peptides associated with the classical MHC Ia molecules, both Qa-1^b and Qa-2^a -associated peptides were longer in ERAAP-deficient cells. Further, some Qa-2^a peptides found exclusively in WT cells are lost in ERAAP-deficient cells, and other novel peptides are associated with Qa-2^a in ERAAP-deficient cells. These results suggest that ERAAP is required for trimming peptides for presentation by Qa-2^a, in a manner similar to its effect on classical MHC Ia molecules.

We observed a striking increase in the number of Qa-1^b -associated peptides specific to ERAAP-deficient cells. We found a total of 153 (67 ERAAP-KO-specific + 86 common) peptides associated with Qa-1^b in ERAAP-deficient cells, compared to a total of 92 in WT cells (6 found only in WT + 86 common). Interestingly, these peptides had a wide distribution of lengths, and showed no clear consensus motif. Instead, Qa-1^b -binding peptides were enriched for a hydrophobic residue at the C-terminus, with no other obvious anchor positions, except a preference for a hydrophobic residue at P3, and a polar residue at P5. Even these preferences are lost in 10-mer peptides, and in peptides from ERAAP-KO

cells. Recent work from Chen et al (40) found a distinct peptide motif in peptides eluted from Qa-1^b -H-$2D^b$ hybrid molecules transduced into human HeLa cells, a motif which we did not observe in this data set. It is possible that differences in peptide isolation methods, and differential affinity of human β_2m (in HeLa cells) and native mouse β_2m could account for these differences.

Strikingly, Qa-1^b was the only MHC I molecule which was associated with a larger number of peptides in the absence of ERAAP. This distinction can perhaps account for why WT CD8 T cells were predominantly specific for the peptide- Qa-1^b repertoire presented by ERAAP-deficient cells, while CD8 T cells in ERAAP-deficient mice responded only to pMHC Ia complexes on WT APCs. While we cannot formally exclude Qa-2^a or other pMHC Ib at this time, the greatly increased numbers of unedited Qa-1^b-associated peptides in ERAAP-deficient cells suggests that altered presentation by Qa-1^b is an important determinant of the immunogenicity of ERAAP-deficient cells. It appears that Qa-1^b occupies a unique niche, presenting a greater number of peptides under conditions of defective antigen processing, such as in the absence of TAP and ERAAP (15, 41). These results strongly suggest that presentation of a wide array of peptides by Qa-1^b serves as a warning for defective antigen processing machinery in the ER.

We have shown before that MHC I-associated peptides are a faithful representation of the cellular state (16, 18, 19). We used gene ontology terms to determine that peptides derived from Golgi-associated genes were specifically enriched in ERAAP-deficient cells. Peptide-MHC I complexes are less stable in ERAAP-deficient cells (13). This instability might make it possible for peptide exchange and loading to occur in post-ER compartments, such as the Golgi, leading to a shift in the sources of peptides. Indeed studies have shown that MHC I molecules can be loaded in post-ER compartments (42, 43).

Another notable change we observed was a specific increase in peptides derived from leucine rich repeat (LRR)—containing proteins in ERAAP-deficient cells. Strikingly, the DA9 peptide, presented exclusively by ERAAP-deficient cells, was derived from the LRR-containing protein Fbxl19. The human *FBXL19* gene, and *ERAP1* (the human ortholog of ERAAP) have both been associated with psoriasis in genome-wide association studies (6, 7). We found that the Fbxl19-derived DA9 peptide was not only presented by ERAAP-deficient cells, but was capable of inducing a CD8+ T cell response in WT mice. Psoriasis is a primarily CD8 T cell-mediated autoimmune disease, although the antigens associated with pathogenic T cells remain unknown (44). While the significance of the *FBXL19*- specific CD8 T cells to psoriasis remains to be determined, our observations provide a potential molecular mechanism for ERAAP-associated autoimmunity.

In summary, we have shown that the loss of ERAAP leads to shifts in the nature and lengths of peptides presented by MHC I molecules on the cell surface. In the absence of ERAAP, MHC Ia and Ib molecules present longer peptides, while a distinct set of ERAAP-edited peptides presented in WT cells is lost. Strikingly, we also find changes in the antigenic precursors from which MHC I-associated peptides are derived, suggesting mechanistic and metabolic changes may occur as a consequence of ERAAP deficiency. We also identified a peptide from an autoimmunity-associated gene that is presented only in the absence of

ERAAP. We suggest that proteomic analyses of MHC I-associated peptides could be useful not only in identifying potential antigenic targets, but also in investigating metabolism and disease-related phenomena.

Supplementary Material

Refer to Web version on PubMed Central for supplementary material.

Acknowledgments

The authors would like to acknowledge Federico Gonzalez, Caroline Côté and the staff of the proteomic core facility at the Institute for Research in Immunology and Cancer for technical assistance and discussions. We thank David King for peptide synthesis.

References

1. Shastri N, Schwab S, Serwold T. Producing nature's gene-chips. The generation of peptides for display by MHC class I molecules. Annu Rev Immunol. 2002; 20:463–493. [PubMed: 11861610]
2. Blum JS, Wearsch PA, Cresswell P. Pathways of antigen processing. Annu Rev Immunol. 2013; 31:443–473. [PubMed: 23298205]
3. Neefjes J, Jongsma ML, Paul P, Bakke O. Towards a systems understanding of MHC class I and MHC class II antigen presentation. Nat Rev Immunol. 2011; 11:823–836. [PubMed: 22076556]
4. de Verteuil D, Granados DP, Thibault P, Perreault C. Origin and plasticity of MHC I-associated self peptides. Autoimmun Rev. 2012; 11:627–635. [PubMed: 22100331]
5. Serwold T, Gonzalez F, Kim J, Jacob R, Shastri N. ERAAP customizes peptides for MHC class I molecules in the endoplasmic reticulum. Nature. 2002; 419:480–483. [PubMed: 12368856]
6. Strange A, Capon F, Spencer CC, Knight J, Weale ME, Allen MH, Barton A, Band G, Bellenguez C, Bergboer JG, Blackwell JM, Bramon E, Bumpstead SJ, Casas JP, Cork MJ, Corvin A, Deloukas P, Dilthey A, Duncanson A, Edkins S, Estivill X, Fitzgerald O, Freeman C, Giardina E, Gray E, Hofer A, Huffmeier U, Hunt SE, Irvine AD, Jankowski J, Kirby B, Langford C, Lascorz J, Leman J, Leslie S, Mallbris L, Markus HS, Mathew CG, McLean WH, McManus R, Mossner R, Moutsianas L, Naluai AT, Nestle FO, Novelli G, Onoufriadis A, Palmer CN, Perricone C, Pirinen M, Plomin R, Potter SC, Pujol RM, Rautanen A, Riveira-Munoz E, Ryan AW, Salmhofer W, Samuelsson L, Sawcer SJ, Schalkwijk J, Smith CH, Stahle M, Su Z, Tazi-Ahnini R, Traupe H, Viswanathan AC, Warren RB, Weger W, Wolk K, Wood N, Worthington J, Young HS, Zeeuwen PL, Hayday A, Burden AD, Griffiths CE, Kere J, Reis A, McVean G, Evans DM, Brown MA, Barker JN, Peltonen L, Donnelly P, Trembath RC. A genome-wide association study identifies new psoriasis susceptibility loci and an interaction between HLA-C and ERAP1. Nature Genetics. 2010; 42:985–990. [PubMed: 20953190]
7. Stuart PE, Nair RP, Ellinghaus E, Ding J, Tejasvi T, Gudjonsson JE, Li Y, Weidinger S, Eberlein B, Gieger C, Wichmann HE, Kunz M, Ike R, Krueger GG, Bowcock AM, Mrowietz U, Lim HW, Voorhees JJ, Abecasis GR, Weichenthal M, Franke A, Rahman P, Gladman DD, Elder JT. Genome-wide association analysis identifies three psoriasis susceptibility loci. Nature genetics. 2010; 42:1000–1004. [PubMed: 20953189]
8. Guerini FR, Cagliani R, Forni D, Agliardi C, Caputo D, Cassinotti A, Galimberti D, Fenoglio C, Biasin M, Asselta R, Scarpini E, Comi GP, Bresolin N, Clerici M, Sironi M. A functional variant in ERAP1 predisposes to multiple sclerosis. PloS ONE. 2012; 7:e29931. [PubMed: 22253828]
9. Keidel S, Chen L, Pointon J, Wordsworth P. ERAP1 and ankylosing spondylitis. Curr Opin Immunol. 2013; 25:97–102. [PubMed: 23452840]
10. Lysell J, Padyukov L, Kockum I, Nikamo P, Stahle M. Genetic association with ERAP1 in psoriasis is confined to disease onset after puberty and not dependent on HLA-C*06. J Invest Dermatol. 2013; 133:411–417. [PubMed: 22931917]
11. Garcia-Medel N, Sanz-Bravo A, Van Nguyen D, Galocha B, Gomez-Molina P, Martin-Esteban A, Alvarez-Navarro C, de Castro JA. Functional interaction of the ankylosing spondylitis-associated

endoplasmic reticulum aminopeptidase 1 polymorphism and HLA-B27 in vivo. Mol Cell Proteomics. 2012; 11:1416–1429. [PubMed: 22918227]

12. Alvarez-Navarro C, Martin-Esteban A, Barnea E, Admon A, Lopez de Castro JA. Endoplasmic Reticulum Aminopeptidase 1 (ERAP1) Polymorphism Relevant to Inflammatory Disease Shapes the Peptidome of the Birdshot Chorioretinopathy-Associated HLA-A*29:02 Antigen. Mol Cell Proteomics. 2015; 14:1770–1780. [PubMed: 25892735]
13. Hammer GE, Gonzalez F, Champsaur M, Cado D, Shastri N. The aminopeptidase ERAAP shapes the peptide repertoire displayed by major histocompatibility complex class I molecules. Nat Immunol. 2006; 7:103–112. [PubMed: 16299505]
14. Hammer GE, Gonzalez F, James E, Nolla H, Shastri N. In the absence of aminopeptidase ERAAP, MHC class I molecules present many unstable and highly immunogenic peptides. Nat Immunol. 2007; 8:101–108. [PubMed: 17128277]
15. Nagarajan NA, Gonzalez F, Shastri N. Nonclassical MHC class Ib-restricted cytotoxic T cells monitor antigen processing in the endoplasmic reticulum. Nat Immunol. 2012; 13:579–586. [PubMed: 22522492]
16. Fortier MH, Caron E, Hardy MP, Voisin G, Lemieux S, Perreault C, Thibault P. The MHC class I peptide repertoire is molded by the transcriptome. J Exp Med. 2008; 205:595–610. [PubMed: 18299400]
17. Mester G, Hoffmann V, Stevanovic S. Insights into MHC class I antigen processing gained from large-scale analysis of class I ligands. Cell Mol Life Sci. 2011; 68:1521–1532. [PubMed: 21387142]
18. de Verteuil D, Muratore-Schroeder TL, Granados DP, Fortier MH, Hardy MP, Bramoulle A, Caron E, Vincent K, Mader S, Lemieux S, Thibault P, Perreault C. Deletion of immunoproteasome subunits imprints on the transcriptome and has a broad impact on peptides presented by major histocompatibility complex I molecules. Mol Cell Proteomics. 2010; 9:2034–2047. [PubMed: 20484733]
19. Caron E, Vincent K, Fortier MH, Laverdure JP, Bramoulle A, Hardy MP, Voisin G, Roux PP, Lemieux S, Thibault P, Perreault C. The MHC I immunopeptidome conveys to the cell surface an integrative view of cellular regulation. Mol Syst Biol. 2011; 7:533. [PubMed: 21952136]
20. Lundegaard C, Lund O, Nielsen M. Accurate approximation method for prediction of class I MHC affinities for peptides of length 8, 10 and 11 using prediction tools trained on 9mers. Bioinformatics. 2008; 24:1397–1398. [PubMed: 18413329]
21. Reche PA, Glutting JP, Zhang H, Reinherz EL. Enhancement to the RANKPEP resource for the prediction of peptide binding to MHC molecules using profiles. Immunogenetics. 2004; 56:405–419. [PubMed: 15349703]
22. Reche PA, Reinherz EL. Prediction of peptide-MHC binding using profiles. Methods Mol Biol. 2007; 409:185–200. [PubMed: 18450001]
23. Huang da W, Sherman BT, Lempicki RA. Systematic and integrative analysis of large gene lists using DAVID bioinformatics resources. Nat Protoc. 2009; 4:44–57. [PubMed: 19131956]
24. Blanchard N, Kanaseki T, Escobar H, Delebecque F, Nagarajan NA, Reyes-Vargas E, Crockett DK, Raulet DH, Delgado JC, Shastri N. Endoplasmic reticulum aminopeptidase associated with antigen processing defines the composition and structure of MHC class I peptide repertoire in normal and virus-infected cells. J Immunol. 2010; 184:3033–3042. [PubMed: 20173027]
25. Joyce S, Tabaczewski P, Angeletti RH, Nathenson SG, Stroynowski I. A nonpolymorphic major histocompatibility complex class Ib molecule binds a large array of diverse self-peptides. J Exp Med. 1994; 179:579–588. [PubMed: 8294869]
26. Tabaczewski P, Chiang E, Henson M, Stroynowski I. Alternative peptide binding motifs of Qa-2 class Ib molecules define rules for binding of self and nonself peptides. J Immunol. 1997; 159:2771–2781. [PubMed: 9300698]
27. Rotzschke O, Falk K, Stevanovic S, Grahovac B, Soloski MJ, Jung D, Rammensee HG. Qa-2 Molecules Are Peptide Receptors of Higher Stringency Than Ordinary Class I Molecules. Nature. 1993; 361:642–644. [PubMed: 8437623]

28. Shastri N, Serwold T, Gonzalez F. Presentation of endogenous peptide/MHC class I complexes is profoundly influenced by specific C-terminal flanking residues. J Immunol. 1995; 155:4339–4346. [PubMed: 7594593]
29. Aldrich CJ, DeCloux A, Woods AS, Cotter RJ, Soloski MJ, Forman J. Identification of a Tap-dependent leader peptide recognized by alloreactive T cells specific for a class Ib antigen. Cell. 1994; 79:649–658. [PubMed: 7525079]
30. Aldrich CJ, Rodgers JR, Rich RR. Regulation of Qa-1 expression and determinant modification by an H-2D-linked gene, Qdm. Immunogenetics. 1988; 28:334–344. [PubMed: 2459056]
31. Jiang H, Chess L. The specific regulation of immune responses by CD8+ T cells restricted by the MHC class Ib molecule, Qa-1. Annu Rev Immunol. 2000; 18:185–216. [PubMed: 10837057]
32. Lo WF, Woods AS, DeCloux A, Cotter RJ, Metcalf ES, Soloski MJ. Molecular mimicry mediated by MHC class Ib molecules after infection with gram-negative pathogens. Nat Med. 2000; 6:215–218. [PubMed: 10655113]
33. Sullivan BA, Kraj P, Weber DA, Ignatowicz L, Jensen PE. Positive selection of a Qa-1-restricted T cell receptor with specificity for insulin. Immunity. 2002; 17:95–105. [PubMed: 12150895]
34. Yan J V, Parekh V, Mendez-Fernandez Y, Olivares-Villagomez D, Dragovic S, Hill T, Roopenian DC, Joyce S, Van Kaer L. In vivo role of ER-associated peptidase activity in tailoring peptides for presentation by MHC class Ia and class Ib molecules. J Exp Med. 2006; 203:647–659. [PubMed: 16505142]
35. Kraft JR, Vance RE, Pohl J, Martin AM, Raulet DH, Jensen PE. Analysis of Qa-1(b) peptide binding specificity and the capacity of CD94/NKG2A to discriminate between Qa-1-peptide complexes. J Exp Med. 2000; 192:613–624. [PubMed: 10974028]
36. Crooks GE, Hon G, Chandonia JM, Brenner SE. WebLogo: a sequence logo generator. Genome Res. 2004; 14:1188–1190. [PubMed: 15173120]
37. Komander D, Rape M. The ubiquitin code. Annu Rev Biochem. 2012; 81:203–229. [PubMed: 22524316]
38. Ghanem E, Fritzsche S, Al-Balushi M, Hashem J, Ghuneim L, Thomer L, Kalbacher H, van Endert P, Wiertz E, Tampe R, Springer S. The transporter associated with antigen processing (TAP) is active in a post-ER compartment. J Cell Sci. 2010; 123:4271–4279. [PubMed: 21098634]
39. Schatz MM, Peters B, Akkad N, Ullrich N, Martinez AN, Carroll O, Bulik S, Rammensee HG, van Endert P, Holzhutter HG, Tenzer S, Schild H. Characterizing the N-terminal processing motif of MHC class I ligands. J Immunol. 2008; 180:3210–3217. [PubMed: 18292545]
40. Chen L, Reyes-Vargas E, Dai H, Escobar H, Rudd B, Fairbanks J, Ho A, Cusick MF, Kumanovics A, Delgado J, He X, Jensen PE. Expression of the mouse MHC class Ib H2-T11 gene product, a paralog of H2-T23 (Qa-1) with shared peptide-binding specificity. J Immunol. 2014; 193:1427–1439. [PubMed: 24958902]
41. Oliveira CC, van Veelen PA, Querido B, de Ru A, Sluijter M, Laban S, Drijfhout JW, van der Burg SH, Offringa R, van Hall T. The nonpolymorphic MHC Qa-1b mediates CD8+ T cell surveillance of antigen-processing defects. J Exp Med. 2010; 207:207–221. [PubMed: 20038604]
42. Garstka M, Borchert B, Al-Balushi M, Praveen PV, Kuhl N, Majoul I, Duden R, Springer S. Peptide-receptive major histocompatibility complex class I molecules cycle between endoplasmic reticulum and cis-Golgi in wild-type lymphocytes. J Biol Chem. 2007; 282:30680–30690. [PubMed: 17656363]
43. Howe C, Garstka M, Al-Balushi M, Ghanem E, Antoniou AN, Fritzsche S, Jankevicius G, Kontouli N, Schneeweiss C, Williams A, Elliott T, Springer S. Calreticulin-dependent recycling in the early secretory pathway mediates optimal peptide loading of MHC class I molecules. Embo J. 2009; 28:3730–3744. [PubMed: 19851281]
44. Nestle FO, Di Meglio P, Qin JZ, Nickoloff BJ. Skin immune sentinels in health and disease. Nat Rev Immunol. 2009; 9:679–691. [PubMed: 19763149]

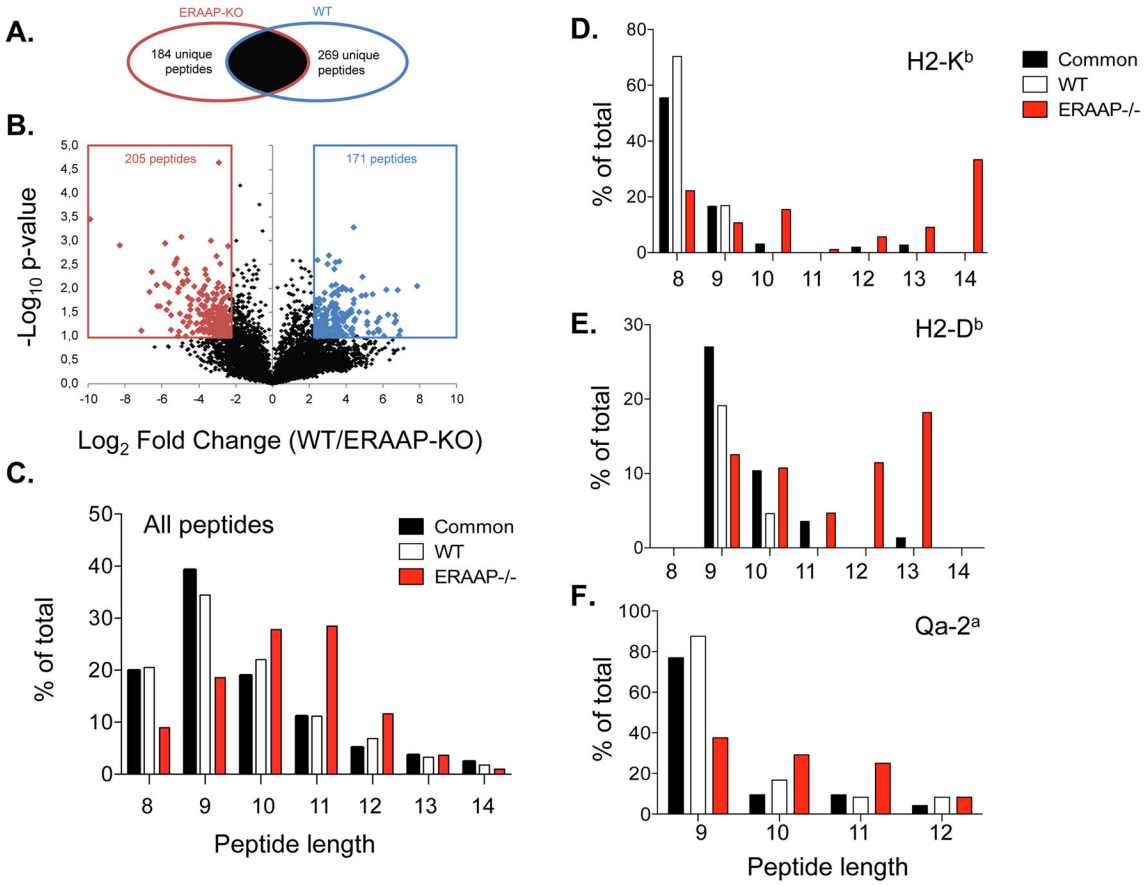

Fig. 1. High throughput mass spectrometry detects unique longer peptides in ERAAP-deficient cells

A. Venn diagrams showing the exclusive and common subsets of peptides found in ERAAP-KO or WT cells. **B.** Volcano plot, showing that common peptides were segregated into ERAAP-KO-specific or WT-specific if they were significantly overexpressed (> 5 fold, $p < 0.1$, two-tailed Student's t test). The numbers indicate different peptides in each category. The average of two independent experiments is shown. **C.** The proportion of peptides of distinct lengths either common to both or specific only to WT or ERAAP-deficient cells. **D,E.** NetMHC was used to identify **D.** H2-K^b- and **E.** H2-D^b-associated peptides with a predicted IC50 of 500nM or higher. **F.** RANKPEP was used to identify Qa-2^a-associated peptides. The lengths of Qa-2^a associated peptides common to both WT and ERAAP-KO cells, or specific to WT or ERAAP-KO cells were compared.

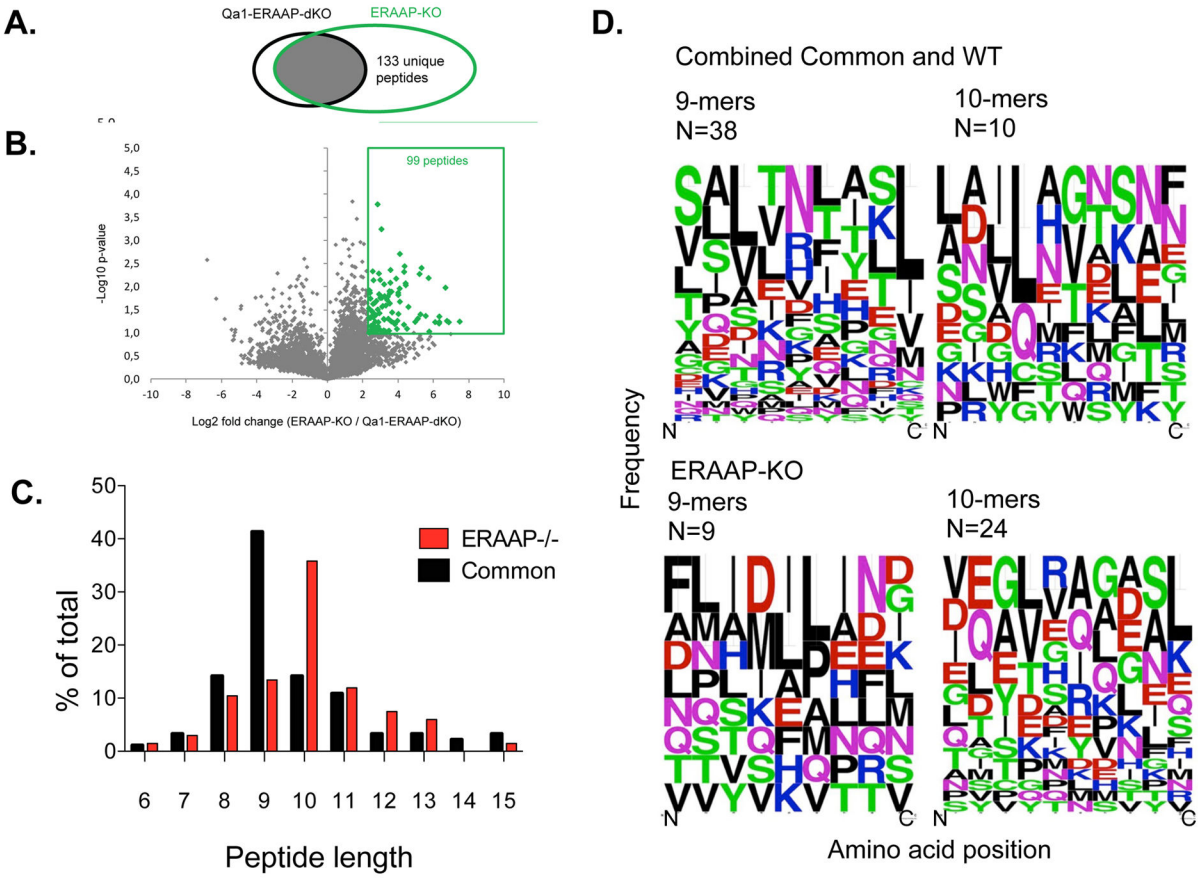

Fig 2. A subtractive approach defines Qa-1^b -associated peptides in ERAAP-deficient cells

A. Venn diagrams showing the subsets of Qa-1^b -associated peptides found in Qa-1^b + ERAAP-KO cells versus Qa-1^b - ERAAP-double KO cells. **B.** Volcano plots, showing that some peptides were significantly over-expressed in ERAAP-KO-cells compared to Qa-1^b - ERAAP-DKO cells (> 5 fold, $p < 0.1$, two-tailed Student's t test). The numbers indicate distinct peptides found in each category. The average of two independent experiments is shown. **C.** The proportion of peptides of distinct lengths either specific to ERAAP-deficient cells, or common to both ERAAP-KO and WT cells. **D.** Weblogo plots, showing the amino acid composition of 9- or 10-reside long Qa-1^b -associated peptides, either specific to ERAAP-deficient cells or common to both ERAAP-deficient and WT cells. Amino acids are represented by their single letter code, and the size of the letter is proportional to the frequency with which that amino acid occurs at the position indicated on the X-axis. The color of the letter indicates the chemical nature of the amino acid as follows: Green-polar, Black-hydrophobic, Red-acidic, Magenta- Blue-basic. N indicates the numbers of peptides in each group.

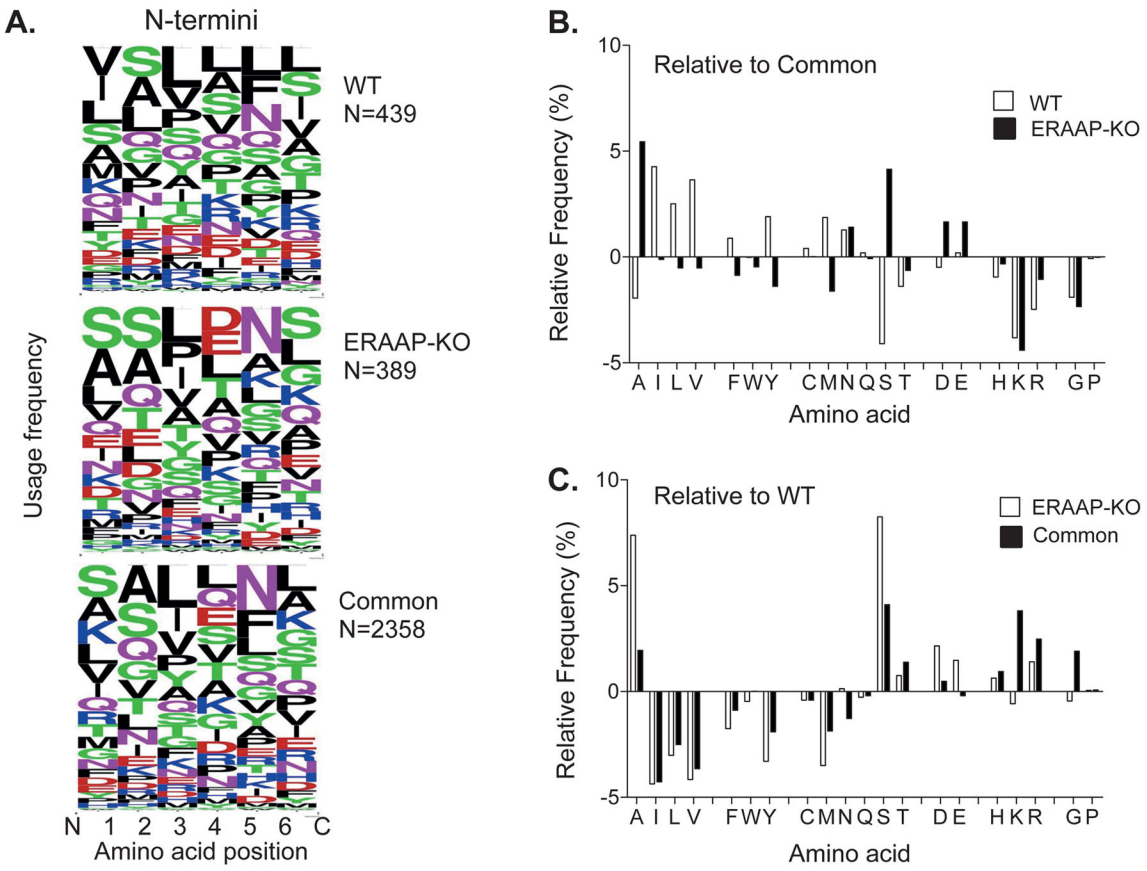

Fig. 3. ERAAP editing results in a unique N-terminal peptide motif

A. Weblogo plots, showing the N-terminal amino acid composition of peptides either specific to WT and ERAAP-deficient cells, or common to both. Amino acids are represented by their single letter symbol, and the size of the letter is proportional to the frequency with which that amino acid occurs at the position indicated on the X-axis. The color of the letter indicates the chemical nature of the amino acid as follows: Green-polar, Black-hydrophobic, Red-acidic Magenta- Blue-basic. N is the numbers of distinct peptides in the group. **B.** The relative frequency of each amino acid at the N-terminal position of WT- and ERAAP-KO-specific peptides was calculated by subtracting the frequency of occurrence of the amino acid at that position in common peptides from the frequency of occurrence in WT- or ERAAP-KO-specific peptides. **C.** The frequency of individual amino acids at the N-terminus of common or ERAAP-KO-specific peptides relative to WT-specific peptides.

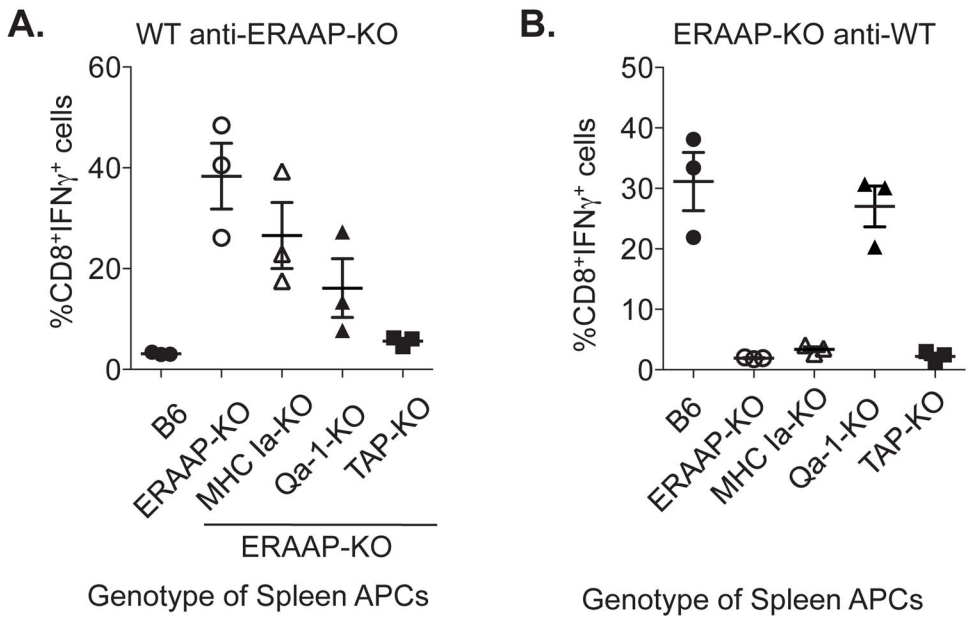

Fig. 4. Differences in specificity of WT anti-ERAAP-ko and ERAAP-KO anti-WT immune responses

A. WT B6 mice were immunized with ERAAP-KO spleen cells, or **B.** ERAAP-KO mice were immunized with WT spleen cells. Spleens from immunized mice were harvested after ten days and restimulated *in vitro* with the same APCs used for immunization. The resulting CD8 T cell responses to the indicated APCs were measured as intracellular IFNγ production. Forward and side scatter were used to exclude dead and granular cells, and the cells in the resulting lymphocyte gate were $B220^{-}CD4^{-}CD8\alpha^{+}TCR\beta^{+}$. Each point represents a different mouse responding to splenic APCs of the indicated genotype. . The data are presented as the mean of five mice, with the bars representing standard error of the mean. When analyzed by non-parametric one way ANOVA (Kruskal-Wallis with Dunn's post-test), the data are statistically significant, with p=0.0157 and p=0.0169 for Fig A and B respectively.

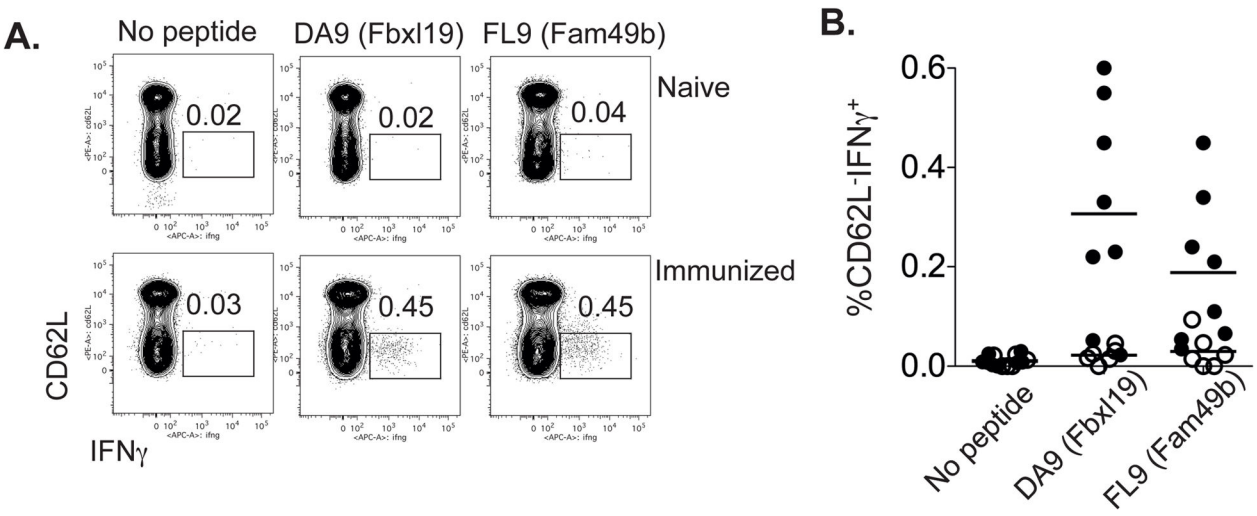

Fig. 5. The *Fbxl19*-encoded DA9 peptide is presented by ERAAP-KO cells to WT CD8 T cells

WT B6 mice were immunized with ERAAP-KO spleen cells, and immune responses to the DA9 and FL9 peptides were measured directly *ex vivo* by intracellular IFNγ staining. Forward and side scatter were used to exclude dead and granular cells, and the cells in the resulting lymphocyte gate were B220-CD4-CD8α+TCRβ+. **A.** Representative flow cytometry plots show CD8 T cells from immunized, but not naïve mice downregulate L-selectin (CD62L) and produce IFNγ when restimulated with either the DA9 or FL9 synthetic peptides. **B.** Fraction of $CD62L^{lo}$ $IFN\gamma^{+}$ cells in naive wild-type mice (open) or immunized with ERAAP-KO cells (closed). Each point represents an individual animal. Results from eight mice, from two pooled experiments are shown, with the bars representing standard error of the mean. When analyzed by non-parametric one way ANOVA (Kruskal-Wallis with Dunn's post-test), the data are statistically significant, with p=0006.

Table I

Summary of MS/MS results[a]

	WT	ERAAP-KO	Common
Total Number of peptides	439	389	2367
Range of lengths	6–20	6–25	5–28
Qa-1 peptides	6	67	86
Qa-2 peptides	29	24	169

[a]The numbers and lengths of the peptides identified by high throughput LC-MS.

Table II

Unique GO terms and keywords[b]

Analysis parameters	Enriched in ERAAP-KO
GO Terms-CC	Golgi apparatus part, protein- DNA complex, Nucleosome
SP-PIR keywords	WD repeat, leucine-rich repeat, methylation

[b] GO terms and protein function keywords that were uniquely associated with ERAAP-KO-specific peptides.